VERSITA

Cent. Eur. J. Chem. • 9(1) • 2011 • 112-118
DOI: 10.2478/s11532-010-0123-y

Central European Journal of **Chemistry**

# Methylcellulose/$SiO_2$ hybrids: sol-gel preparation and characterization by XRD, FTIR and AFM

**Research Article**

Nadezhda Rangelova[1*], Lachezar Radev[1], Sanchi Nenkova[1], Isabel M. Miranda Salvado[2], Maria H. Vas Fernandes[2], Michael Herzog[3]

[1]*University of Chemical Technology and Metallurgy, 1756 Sofia, Bulgaria*

[2]*University of Aveiro, CICECO, 3810-193 Aveiro, Portugal*

[3]*University of Applied Sciences, 15745 Wildau, Germany*

**Received 12 July 2010; Accepted 29 September 2010**

**Abstract:** Methylcellulose (MC) / $SiO_2$ organic / inorganic hybrid materials have been prepared from MC and methyltriethoxysilane or ethyltrimethoxysilane, and characterized by XRD, FTIR and AFM. XRD showed peak shifts. FTIR shows intermolecular hydrogen bonding between MC and $SiO_2$. AFM depicts surface roughness which depends on the silica precursor and MC content.

**Keywords:** *Methylcellulose • MTES • ETMS • Sol-gel • Hybrids*



## 1. Introduction

Sol-gel methods have been widely applied [1-3]. The sol-gel reaction can be divided into the following steps: (1) alkoxysilane hydrolysis; (2) condensation of hydrated silica to form siloxane (≡Si-O-Si≡), and (3) polycondensation by linkage of additional silanols to cyclic oligomers. The product properties can be altered by a number of factors including pH, temperature, reagent concentrations, reaction time, rates of hydrolysis and condensation, catalyst, *etc*. [4].

Organic / inorganic hybrids are a relatively new type of composite with interesting mechanical, optical, electrical and thermal properties, which arise from the combination of organic polymers and inorganic minerals. A simple preparation method is to mix an organic polymer with a silicon alkoxide such as tetraethoxysilane (TEOS) or tetramethoxysilane (TMOS) followed by sol-gel reaction with a small amount of acid or base catalyst under mild conditions. Hydrogen bonding between the organic polymer and the inorganic mineral plays an important role in avoiding phase separation and yielding transparent free standing films [5]. Such hybrids are promising materials for various applications: solid-state lasers, optical materials, biocatalysts, and anti-corrosion and scratch resistant coatings [6-10].

Methylcellulose is one of the simplest cellulose derivates [11]. It has excellent film and emulsion forming ability with $TiO_2$ and $SiO_2$ [12-15], proteins (β-lactoglobulin and β-casein [16]), molecular sieves (montmorillonite [17] and AlSBA-15 [18]), chitosan [19-21], alginates [22], and some metal ions [23]. It shows cell attachment [24,25], lipid barrier function and a low oxygen transmission rate [26,27]. It has been extensively used in the food [26,28,29], pharmaceutical [20,30,31] and tissue engineering [30,32-34] industries.

We previously investigated the synthesis of hybrid materials containing MC and $SiO_2$ using tetraethylorthosilicate (TEOS) or methyltriethoxysilane (MTES) [35,36]. We observed that $SiO_2$ hybrids obtained from MTES are more stable than these obtained from TEOS [35]. MC / $SiO_2$ hybrids obtained from MTES or ETMS were successfully used as immobilization matrices for the filamentous yeast *Trichosporon cutaneum* strain R57. These were used in cadmium and copper sorption from waste water [36].

The main purpose of the present study was to obtain new MC / SiO2 organic/inorganic hybrids using two different silica precursors (MTES and ETMS), and to investigate their structural characteristics via XRD, FTIR and AFM.

* *E-mail: nadezhda_rangelova@abv.bg*

# 2. Experimental Procedure

The hybrid materials were produced using MC, MTES or ETMS, which belong to the family of organosiloxanes of the type $R_nSiO_{(4-n)/2}$, where R=alkyl group and n=1-3.

The structure of the hybrid materials obtained depends on: (1) the type of R and (2) the R/Si ratio. The R/Si ratio and $SiO_2$ content are given by the reactions:

$$R_nSiX_{4-n} \rightarrow R_nSi(OH)_{4-n} \rightarrow R_nSiO_{(4-n)/2},$$

where R=alkyl, X=alkoxy and n=1-3, given by Rao *et al*. [37].

## 2.1. Materials

Pure MC (average Mw~ 86 000) from Sigma-Aldrich was used without further purification. MTES and ETMS were used as silica precursors. $C_2H_5OH$ and HCl were purchased from Merck. Distilled water was used for hydrolysis and HCl (37%) as catalyst.

## 2.2. Hydrolysis of MTES and ETMS

MTES or ETMS were added to $C_2H_5OH$ and $H_2O$ to form a solution in the molar ratio MTES (ETMS):$C_2H_5OH$:$H_2O$ = 1 (1) : 1 : 3.3. In this system, the hydrolysis reaction is moderate when the molar ratio HCl:MTES (ETMS) is about 0.01. The hydrolysis reaction was conducted at room temperature under intense stirring at 25°C for 1 hour at pH ~2 for each silica precursor. The reaction mixture was transparent and homogeneous during the whole process. The solution obtained is denoted Sol A.

## 2.3. Preparation of MC solution

MC solutions (5 wt%, 20 wt% and 50 wt%), were prepared by dissolving of 0.06750 g, 0.2720 g or 0.6750 g MC in 15 ml cold distilled water under stirring at room temperature. The transparent, homogeneous solution was denoted Sol B.

## 2.4. Hybrid preparation

Sol B was slowly added to Sol A under magnetic stirring for 2 hours. The Sol C obtained was also transparent and homogeneous. Gelation and drying were carried out at 50°C for 12 h.

The MC / $SiO_2$ hybrid synthesis pathway is given in Scheme 1.

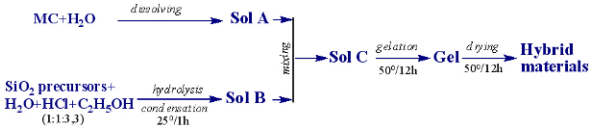


**Scheme 1.** Sol-gel synthesis of MC / $SiO_2$ hybrids.

## 2.5. Characterization methods

The MC / $SiO_2$ hybrid structures were examined by X-ray diffraction (XRD) analysis, Fourier-transform infrared (FTIR) spectroscopy and atomic force microscopy (AFM).

Powder XRD spectra were collected from 2θ = 4° to 80° with a constant 0.02° 2θ step at 1s/step using a Bruker D8 Advance diffractometer with $CuK_\alpha$ radiation and SolX detector. The spectra were evaluated with the Diffrac*plus* EVA package.

FTIR transmission spectra were recorded on a Bruker Tensor 27 spectrometer with scanning velocity 10KHz, using an MCT detector, with 64 scans and 1 $cm^{-1}$ resolution. KBr pellets were prepared by mixing ~1 mg of the samples with 300 mg KBr.

AFM images were taken in air at room temperature with a NT-MDT SOLVER equipped with a NSG01 cantilever (Golden Silicon Probes).

# 3. Results and Discussion

## 3.1. FTIR of methylcellulose (MC)

Fig. 1 depicts the FTIR spectrum of pure MC.

As can be seen, pure MC had O-H stretching vibrations at 3459 $cm^{-1}$ [17,38-40]. C-H stretching at 2932 and 2843 $cm^{-1}$ [17,38,40-42]. C-O carbonyl stretching from the glucose in the cellulose at 1647 $cm^{-1}$ overlaps adsorbed water [17,40,42,43]. C-O stretching from the asymmetric oxygen bridge at 1126 $cm^{-1}$ and ring stretching at 945 $cm^{-1}$ are in the "fingerprint region" [38,40,43,44]. Moreover, the spectrum also showed characteristic cellulose peaks in the range 1000-1200 $cm^{-1}$. The 1126 $cm^{-1}$ peak was ascribed to the asymmetric C-O-C stretch [40,44]. The 1379 $cm^{-1}$ peak corresponds to MC C-H bending [40]. In agreement with Filho *et al*. [41] we also observe the MC bands at 1460, ~1380, ~1320 and 950 $cm^{-1}$. On the other hand, we did not observe the bands at 1730, 1620, 1595 and 1512 $cm^{-1}$ [42] as the MC used was purified.

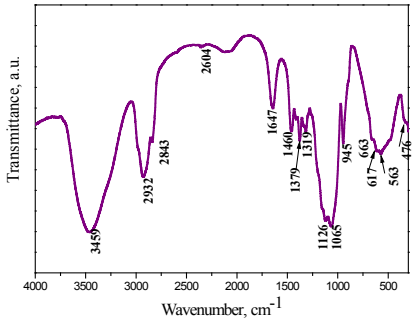


**Figure 1.** FTIR spectrum of pure MC.

## 3.2. FTIR of $SiO_2$ (MTES) and $SiO_2$ (ETMS), prepared via the sol-gel method.

The FTIR spectra of sol-gel $SiO_2$ from MTES or ETMS produced at 25°C and dried at 50°C for 12 h are shown in Fig. 2.

The FTIR spectra of the dried silica gels obtained from MTES or ETMS show common bands. Fig. 2, curves 1 and 2 showed a broad band centered at 3454 (3465) $cm^{-1}$ due to overlap of the OH stretchings of hydrogen bonded $H_2O$ and surface Si-OH hydrogen-bonded to water [45,46]. The Si-O stretching of Si-OH appears at 908 $cm^{-1}$ [46,47] and adsorbed $H_2O$ at 1651-1639 $cm^{-1}$ [47,48], $H_2O$ adsorption can be considered to measure the materials' hydrophobicity. Intense Si-O vibrations appear mainly in the 1007 $cm^{-1}$ (curve 1) – 1158 $cm^{-1}$ (curve 2) range showing dense silica structures, where oxygen bridges two silicon sites [37,46,49-51]. In the case of ETMS (curve 1) the 1046 $cm^{-1}$ band was attributed to the C-C-O vibrations of $C_2H_5OH$ [47]. This band overlapped Si-O-Si of condensed silicate. The Si-O-Si bending mode appears at 446 (435) $cm^{-1}$ [49]. The low energy band at 557 (579) $cm^{-1}$ could be assigned to Si-O stretching of $SiO_2$ network defects [45]. From Fig. 2, curve 1 shows the presence of C-H stretching at 2973 and 2887 $cm^{-1}$ and C-H deformation at 1468 $cm^{-1}$ [45]. The 1257 $cm^{-1}$ C-H bend [45,46,48,49,52] is less intense than that of MTES at 1289 $cm^{-1}$ (curve 2). This decrease could be due to steric hindrance of the $C_2H_5$ group in ETMS compared to the $CH_3$ group in MTES [45]. The bands at 888 and 755 $cm^{-1}$ (curve 1) and a band at 777 $cm^{-1}$ (curve 2) could be ascribed to Si-C [45]. Some authors assumed that the peaks I at ~1270 and ~2970 $cm^{-1}$ are from Si-C bonds and $-CH_3$ from the silica precursor in the mixed sol [53]. Further, the 690 $cm^{-1}$ (curve 1) and 908 $cm^{-1}$ (curve 2) peak are assigned to the Si-O symmetric stretch and to the Si-O- in-plane stretch [45].

## 3.3. FTIR of the synthesized hybrids

FTIR spectra were obtained to examine interactions between $SiO_2$ and MC. Results are in Figs. 3 and 4.

Comparing the FTIR spectra of pure MC (Fig. 1), $SiO_2$ (Fig. 2) and MC / $SiO_2$ (MTES or ETMS) hybrids (Figs. 3 and 4), the pure MC and $SiO_2$ peaks all appear in the hybrids' spectra except for slight band shifts. FTIR shows no significant change of the two components after hybrid preparation. However, increasing gelation temperature from 25 to 50°C causes significant change in the OH stretching and bending peaks at 3459 and 1647 $cm^{-1}$ (Fig. 1). The 3459 $cm^{-1}$ peak for pure MC

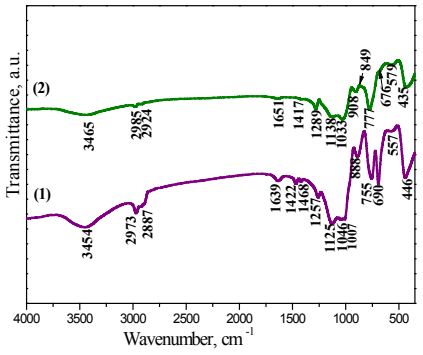


**Figure 2.** FTIR spectra of dried $SiO_2$ from (1) ETMS, and (2) MTES.

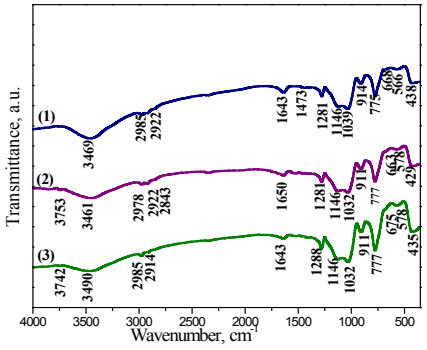


**Figure 3.** FTIR spectra of MC / $SiO_2$ (MTES) hybrids: (1) 5 wt%; (2) 20 wt%; (3) 50 wt% MC.

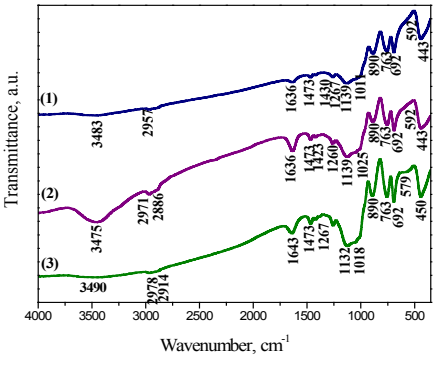


**Figure 4.** FTIR spectra of MC / $SiO_2$ (ETMS) hybrids: (1) 5 wt%; (2) 20 wt%; (3) 50 wt% MC.

shifted to ~3440 $cm^{-1}$ for the MTES hybrids (Fig. 3) and ~3475 $cm^{-1}$ for the ETMS hybrid (Fig. 4). At the same time, the 1647 $cm^{-1}$ peak slightly shifted by ~10 $cm^{-1}$ and decreased in intensity in the hybrids. These shifts suggest intermolecular hydrogen bonding, similar to other hybrids [39,40,43,54-57].

Scheme 2 shows a plausible way of linking MC and $SiO_2$.

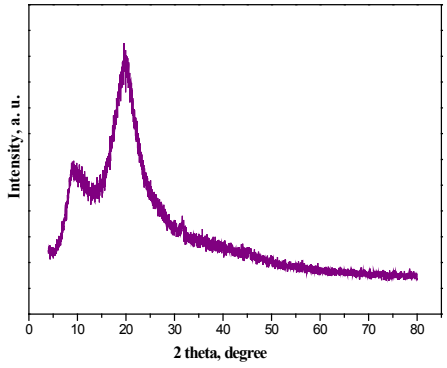


**Figure 5.** XRD of pure MC.

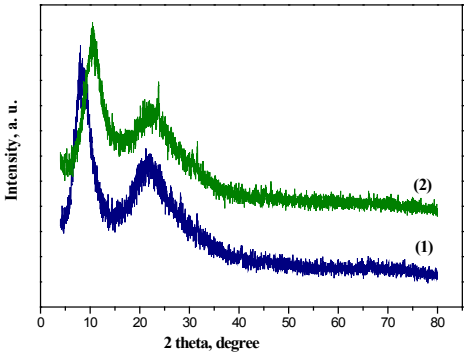


**Figure 6.** XRD of silica, obtained from hydrolyzed (1) ETMS and (2) MTES.

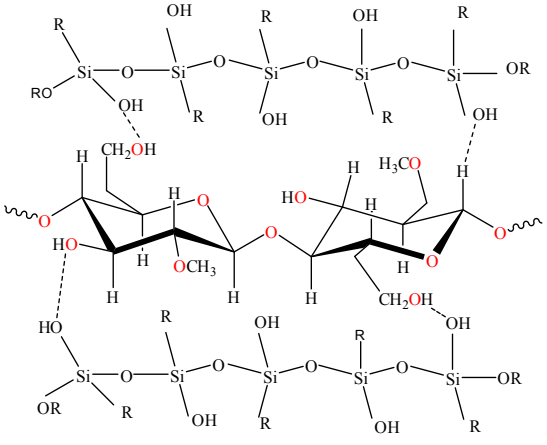

**Scheme 2.** Possible interactions between methylcellulose and silica derived from organosiloxanes

## 3.4. X-ray diffraction data for the hybrids.

Figs. 5 and 6 present X-ray diffraction data of pure MC and for hydrolyzed pure silicate precursors MTES and ETMS.

X-ray diffraction for pure MC (Fig. 5) showed a semicrystalline structure. The patterns exhibited a sharp peak at 2θ=8.9° and a broad peak centered at 2θ=19.8°. In agreement with Pinotti *et al*. [19], we ascribe the 8.9° peak to glucose-type crystalline order in the MC. Rimdusit *et al*. [17] concluded that peaks at 2θ=9-21° indicate the intermolecular structure of the MC. Others postulated that the 2θ=8° peak represents the degree of cellulose modification [41]. On the other hand, silica obtained from both precursors (Fig. 6) exhibited typical diffraction patterns associated with amorphous silica [58].

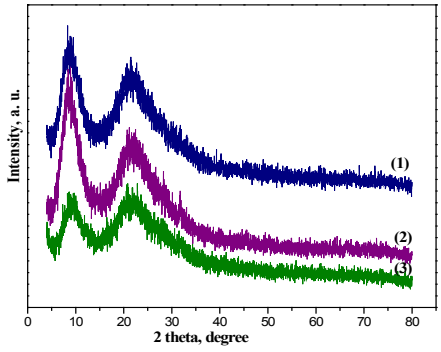


**Figure 7.** XRD for the MC / $SiO_2$ (MTES) hybrids: (1) 5 wt%, (2) 20 wt%, and (3) 50 wt%.

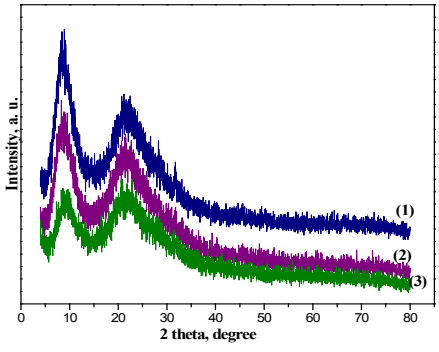


**Figure 8.** XRD for the MC / $SiO_2$ (ETMS) hybrids: (1) 5 wt%, (2) 20 wt%, and (3) 50 wt%.

**Table 1.** Position of the peaks maximum of the precursors and the synthesized hybrids.

| Sample | Figure, (curve) | Peak maximum (2θ, degrees) | |
|---|---|---|---|
| | | First | Second |
| **MC** | 5 | 8.93 | 19.89 |
| **ETMS** | 6 (1) | 8.03 | 21.69 |
| **MTES** | 6 (2) | 10.57 | 22.28 |
| **MTES-5 wt% MC** | 7 (1) | 8.91 | 21.81 |
| **MTES-20 wt % MC** | 7 (2) | 8.58 | 21.64 |
| **MTES-50 wt% MC** | 7 (3) | 8.91 | 21.31 |
| **ETMS-5 wt% MC** | 8 (1) | 8.58 | 21.81 |

The hybrid materials' XRD data are presented in Figs. 7 and 8.

XRD patterns of the hybrids are similar to those for pure MC and silica from the precursors. Two similar peaks are observed for the hybrid materials containing up to 50 wt% MC. Figs. 7 and 8 show that the intensity

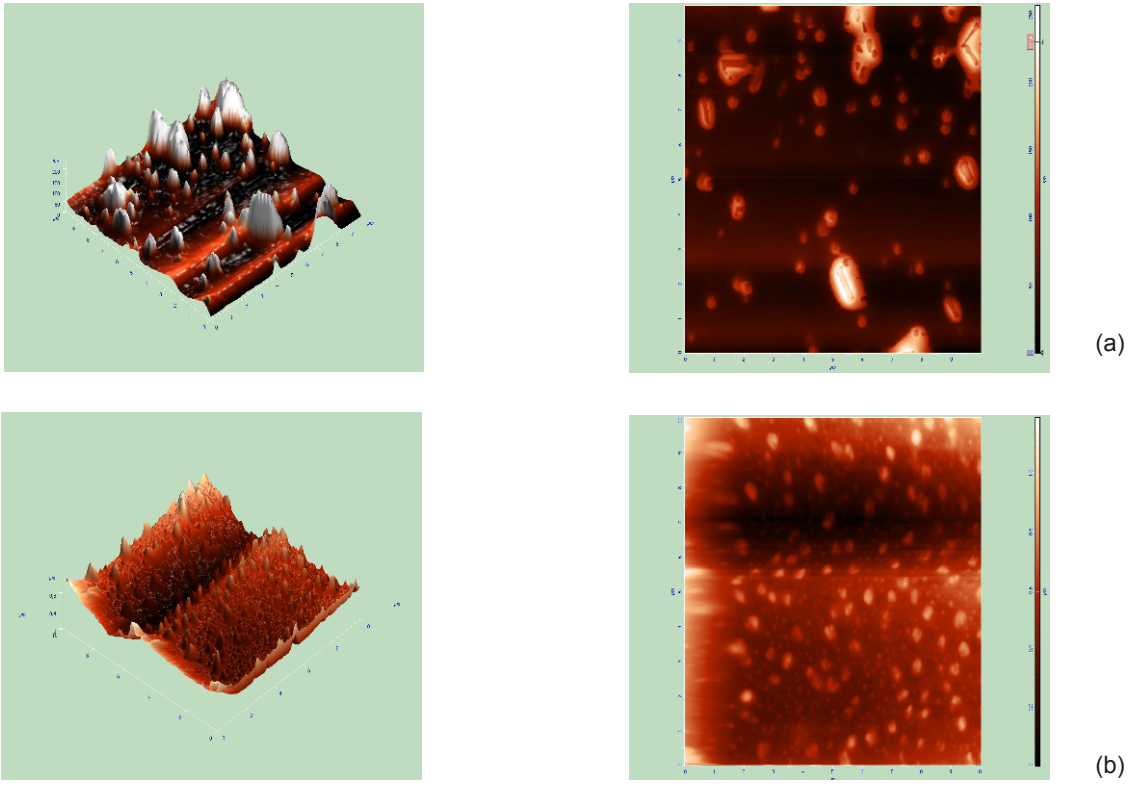


**Figure 9.** AFM images of MC / $SiO_2$ (MTES) hybrids: (a) 5 wt% MC; (b) 50 wt% MC.

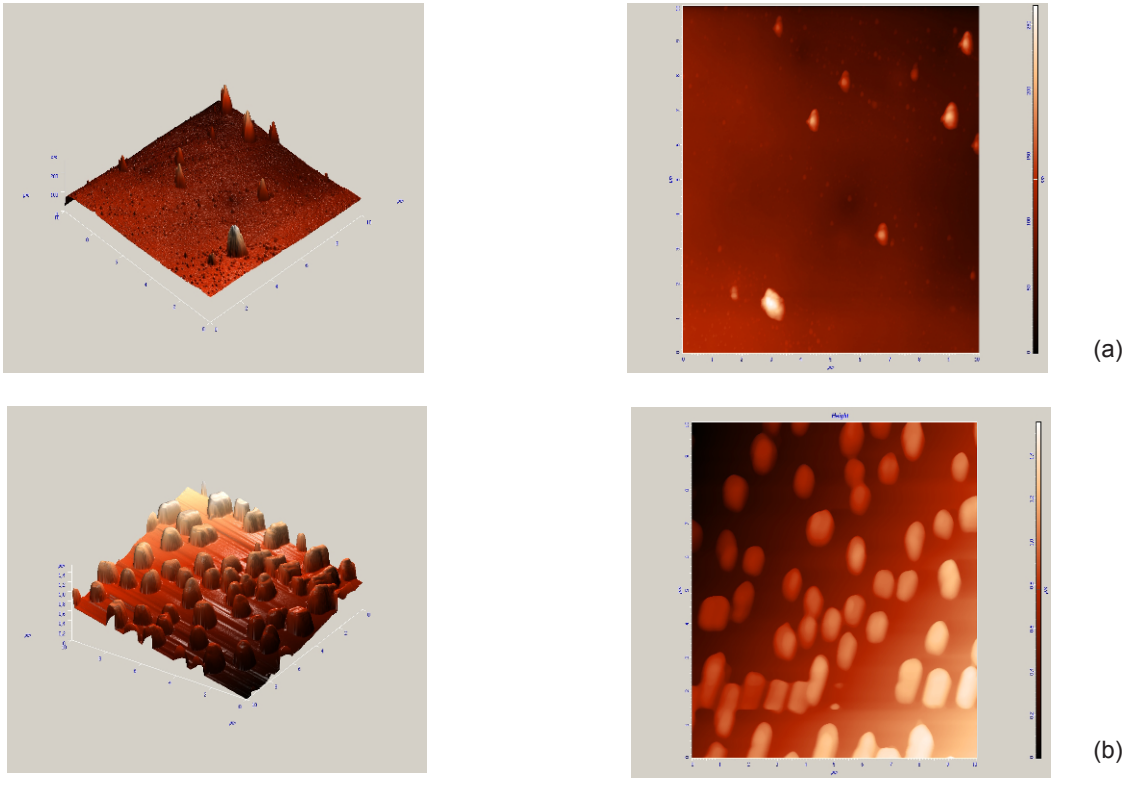


**Figure 10.** AFM images of MC / $SiO_2$ (ETMS) hybrids: (a) 5 wt% MC; (b) 50 wt% MC.

of the peaks decreases with increasing initial MC. Yano *et al*. [59] and Wojciechowski [60] observed the same dependence on silica content for HPC / silica hybrids. They concluded that HPC molecules are incorporated into the silica network. HPC crystallites may have formed in the hybrids' HCP-rich phase.

The changes of peak position in the hybrids compared with those in pure MC (Fig. 5) and MTES or ETMS (Fig. 6, curves 1 and 2) are summarized in Table 1.

The 2θ values differ between the hybrids. Similar results have been reported [17,19,61]. We hypothesize that the hybrids are produced after formation of the hydrogen bonds and electrostatic interactions between the two components.

Figs. 9 and 10 depict AFM surface topography images of the MC / $SiO_2$ hybrids.

AFM showed mesopores in the range of 2 - 2.5 μm, probably due to water and solvent (alcohol) vapor release during drying. AFM also showed that MC content and silica precursor influence not only the chemical nature of the hybrids, but also the surface morphology. The 50 wt% MC / $SiO_2$ (MTES) shown in Fig. 9b was very uniform and smooth, while large particles (mostly globular) were found in 50 wt% MC / $SiO_2$ (ETMS) in Fig. 10b. With higher MC content larger aggregates can be observed with ETMS as silica precursor. The surface has many islands dispersed on the silica surface. In the case of MTES with higher MC content (Fig. 9b) the surface roughness increased dramatically and small aggregates (0.1 to 0.6 μm) were observed. This increased surface roughness depends on the silica precursor and MC content.

## 4. Conclusions

The aim of the present article was to prepare MC / $SiO_2$ hybrid materials containing varying amounts of MC. The materials were characterized by XRD, FTIR and AFM.

XRD showed that the peak intensities decrease with increasing initial MC content.

FTIR showed that with the increase in gelation temperature from 25 to 50°C, the 3459 and 1647 $cm^{-1}$ OH stretching and bending peaks change significantly. The 3459 $cm^{-1}$ peak for pure MC shifted to ~3440 $cm^{-1}$ for MTES hybrids and to ~3475 $cm^{-1}$ for ETMS hybrids. The 1647 $cm^{-1}$ peak slightly shifted by ~10 $cm^{-1}$ and decreased in intensity in the hybrids. These shifts suggest the formation of intermolecular hydrogen bonds.

AFM shows that with higher MC content larger aggregates form using ETMS. For MTES with higher MC content the surface roughness increased dramatically. Increased surface roughness thus depends on the silica precursor and the MC content.

Future work will examine the usefulness of MC/$SiO_2$ hybrids as drug carriers.

## References


[1] W. Cuiming, X. Tongwen, Y. Weihua, Journal of Membrane Science 216, 269 (2003)
[2] Y. Shchipunov, Journal of Colloid and Interface Science 268, 68 (2003)
[3] M. Kato, K. Sakai- Kato, T. Togo`oka, J. Sep. Sci. 28, 1893 (2005)
[4] S. Yano, K. Iwata, K. Kurita, Materials Science and Engineering C 6, 75 (1998)
[5] S. Li, M. Liu, Electrochimica Acta 48, 4271 (2003)
[6] M. Sheffer, A. Groysman, D. Mandler, Corrosion Science 45, 2893 (2003)
[7] N. Voevodin, et al., Progress in Organic Coatings 47, 416 (2003)
[8] S. Hofacker, et al., Progress in Organic Coatings 45, 159 (2002)
[9] M. Kato, K. Sakai-Kato, T. Toyo'oka, J. Sep. Sci. 1893 (2005)
[10] C. Sanchez, et al., Journal of Material Chemistry 15, 3559 (2005)
[11] H. Kamitakahara, et al., Cellulose 15, 797 (2008)
[12] W. Chen, et al., J. Am. Ceram. Soc. 88[11], 2998 (2005)
[13] M. Habibi, M. Nasr-Esfahani, Dyes and Pigments 75, 714 (2007)
[14] M. Habibi, M. Nasr-Esfahani, T. Egerton, J. Mater. Sci. 42, 6027 (2007)
[15] W. Chen, et al., Sensors and Actuators B. 100, 195 (2004)
[16] J.-C. Arboleya, P. J. Wilde, Food Hydrocolloids 19, 485 (2005)
[17] S. Rimdusit, et al., Carbohydrate Polymers 72, 444 (2008)
[18] G. Chandrasekar, et al., Catalysis Communications 8[3], 457 (2007)
[19] A. Pinotti, et al., Food Hyrocolloids 21, 66 (2007)
[20] A.P. Rokhade, et al., Carbohydrate Polymers 69, 678 (2007)
[21] M.A. Garcıa, et al., Food Hydrocolloids 23 722 (2009)
[22] V.R. Babu, et al., Carbohydrate Polymers 69, 241 (2007)
[23] D.W. O'Connell, C. Birkinshaw, T.F. O'Dwyer, Bioresource Technology 99, 6709 (2008)
[24] S. Yokota, T. Kitaoka, H. Wariishi, Carbohydrate

Polymers 74, 666 (2008)
[25] C.H. Chen, et al., Biomacromolecules 7[3], 736 (2006 )
[26] M.B. Perez-Gago, J. M. Krochta, J. Agric. Food Chem. 48[7], 2687 (2000)
[27] J.A. Ball, PhD Thesis, Blacksburg, Virginia, USA, (1999)
[28] S. Farris, et al., Trends in Food Science & Technology 20, 316 (2009)
[29] T. Bourtoom, International Food Research Journal 15[3], 237 (2008)
[30] E. Reverchon, et al., J. of Supercritical Fluids 47, 484 (2009)
[31] T. Ozeki, H. Yuasa, H. Okada, AAPS PharmSciTech 6[2], E231-E236 ( 2005)
[32] C. Tsioptsias, et al., Materials Science and Engineering C 29, 159 (2009)
[33] P.B. Malafaya, G.A. Silva, R.L. Reis, Advanced Drug Delivery Reviews 59, 207 (2007)
[34] S.S. Stalling, S.O. Akintoye, S.B. Nicoll, Acta Biomaterialia 5 1911 (2009)
[35] N. Rangelova, et al., 16-th Conference on Glass Ceramics, Varna in press (2008)
[36] N. Rangelova, et al., BIO Automation 13[4], 221 (2009)
[37] A.V. Rao, R.R. Kalesh, Sci. J. Adv. Technol. 4, 509 (2003)
[38] Y. Horikawa, T. Itoh, J. Sugiyama, Cellulose 13, 309 (2006)
[39] P. Shi, Y. Li, L. Znang, Carbohydrate Polymers 72, 490 (2008)
[40] S -Y. Lin, et al., Surf. Sci. 601, 781 (2007)
[41] G.R. Filho, et al., Polym. Degrad. and Stab. 92, 205 (2007)
[42] R.G.P. Viera, et al., Carbohydrate Polymers 67, 182 (2007)
[43] M. Tsuboi, J. Polym. Sci. XXV, 159 (1957)
[44] D.K. Buslov, N.I. Sushko, O.N. Tretinnikov, J. Appl. Spectroscopy 75 [4], 514 (2008)
[45] R. Al-Oweini, H. El-Rassy, J. Mol. Structure 919, 140 (2009)
[46] G. Celichowski, et al., Tribology Letters 14 [3], 181 (2003)
[47] H. Jiang, Z. Zheng, X. Wang, Vibrational Spectroscopy 46, 1 (2008)
[48] D.Y. Nadargi, et al., Microporous and Mesoporous Materials 117, 617 (2009)
[49] A. Phanasgaonkar, V.S. Raja, Surface & Coatings Technology 204, 2260 (2009)
[50] N.D. Hegde, H. Hirashima, A.V. Rao, J. Porous Mater. 14, 165 (2007)
[51] A. Anderson, et al., J. Sol-Gel Sci. Technol. in press, (2009)
[52] T. Oh, Bull. Korean Chem. Soc. 28 [9], 1588 (2007)
[53] T.-J. Ha, et al., 34, 947 (2008)
[54] H.S. Barud, et al., J. Sol-Gel Sci. Technol. 46, 363 (2008)
[55] M. Kusabe, et al., J. Sol-Gel Sci. Technol. 44, 111 (2007)
[56] L. Jiang, et al., Carbohydrate Polymers 74, 680 (2008)
[57] S. Sequeira, et al., Materials Science and Engineering C 27, 172 (2007)
[58] Y. Zhang, et al., J. of Non-Cryst. Solids 351, 777 (2005)
[59] S. Yano, Polymer 35[25], 5565 (1994)
[60] P. Wojciechowski, T. Halamus, U. Pietsch, Materials Science-Poland 24[2/2], (2006)
[61] L. Wang, Y. Xu, Cellulose 13, 191 (2006)